Cronfa - Swansea University Open Access Repository

_____

This is an author produced version of a paper published in:
Mechanical Systems and Signal Processing

_____

Cronfa URL for this paper:

http://cronfa.swan.ac.uk/Record/cronfa35620

_____

Paper:

_____

http://www.swansea.ac.uk/library/researchsupport/ris-support/

Estimation of beam material random field properties via sensitivity-based model updating using experimental frequency response functions

M.R. Machado[a], S. Adhikari[b], J.M.C. Dos Santos[c], and J.R.F. Arruda[c]

[a] *Department of Mechanical Engineering, University of Brasilia - UnB, 70900, Brasilia, Brazil*

[b] *School of Engineering, Swansea University, Singleton Park, Swansea SA2 8PP, UK*

[c] *Department of Computational Mechanics, University of Campinas - UNICAMP, 13083-970, Campinas, SP, Brazil*

Abstract

Structural parameter estimation is affected not only by measurement noise but also by unknown uncertainties which are present in the system. Deterministic structural model updating methods minimise the difference between experimentally measured data and computational prediction. Sensitivity-based methods are very efficient in solving structural model updating problems. Material and geometrical parameters of the structure such as Poisson's ratio, Young's modulus, mass density, modal damping, etc. are usually considered deterministic and homogeneous. In this paper, the distributed and non-homogeneous characteristics of these parameters are considered in the model updating. The parameters are taken as spatially correlated random fields and are expanded in a spectral Karhunen-Loève (KL) decomposition. Using the KL expansion, the spectral dynamic stiffness matrix of the beam is expanded as a series in terms of discretized parameters, which can be estimated using sensitivity-based model updating techniques. Numerical and experimental tests involving a beam with distributed bending rigidity and mass density are used to verify the proposed method. This extension of standard model updating procedures can enhance the dynamic description of structural dynamic models.

Keywords: Parameter estimation, Sensitivity-based model updating, Random

field.

1. Introduction

Quantifying uncertainty in numerically simulated results is not recent. However, during the last few years, this research area has undergone remarkable development, in special for dynamic systems. The method most used is Monte Carlo (MC) simulation [1]. Otherwise, non-sampling approaches such as the Perturbation Method may be used. It consists of expanding a random field in a truncated Taylor series around its mean [2]. The Direct Method consists in applying the moment equations to obtain the random solutions. The unknowns are the moments and their equations are derived by taking averages over the original stochastic governing equations. A powerful method in computational stochastic problems is the Stochastic Finite Element Method (SFEM) [3]. SFEM is an extension of the classical deterministic FE approach to the stochastic framework, i.e., to solve static and dynamic problems with stochastic mechanical, geometric, or loading properties [4]. Adhikari [5] presented a doubly Spectral Stochastic Finite Element Method, where the Spectral Element Method is given a stochastic treatment.

The spectral element method (SEM) [6, 7] is based on the analytical solution of the displacement wave equation, written in the frequency domain. The element is tailored with the matrix ideas of FEM, but in SEM the interpolation function is the exact solution of the wave equation [8, 9, 10, 11, 12, 13, 14, 15, 16, 17, 18, 19, 20]. Both techniques, SFEM and doubly Spectral SFEM, are formulated in a context of random fields. A method with a wide application when considering random fields is the Karhunen-Loève (KL) expansion [3, 21, 2]. The KL expansion can be used to discretize the random field by representing it by scalar independent random variables and continuous deterministic functions. By truncating the expansion, the number of random variables becomes finite and numerically treatable. Many authors use the KL expansion to model Gaussian random processes, but it is possible to extend the KL expansion to

2

non-Gaussian processes [22, 23, 24, 25].

Model updating methods in dynamic structural analysis are basically a process of minimizing the differences between the numerical model predictions and measured responses obtained in experimental tests using a parameter estimation procedure [26, 27]. The model updating procedure starts with the parameter choice (parametrisation), followed by a correction procedure based on the available measured data. The parametrisation is an important topic in model updating which requires considerable physical knowledge regarding the system. More details can be found in references [28, 29, 30, 31, 32]. In the field of structural dynamics, some authors traditionally use modal parameters (natural frequencies and mode shapes) for updating the model due to the facility in estimating the modal parameters using modal analysis [33, 34] and also to the freedom in the choice of the updating parameters and the applicability of the method [35]. Examples of theoretical and practical applications can be found in references [36, 27, 37, 38, 32]. However, in a structural dynamic test, it is a common practice to measure the data in the form of Frequency Response Functions (FRF), which requires an additional modal parameter estimation [33, 39] to extract the modal parameters. Natke [40] presented a model updating procedure using measured FRFs instead of modal parameters. After that, a growing number of researchers focused on model updating algorithms using the measured data directly [41, 42, 43, 44, 45, 46, 47]. In the practical applications of model updating, the measured data are often incomplete and include randomness. Based on the system variability, some authors proposed stochastic model updating techniques [48, 49, 50, 51]. The main advantage of this approach is to add randomness in the model updating process. Statistical techniques combined with model updating can improve the parameter estimation. The first works that incorporated statistical methods for the treatment of measurement noise in model updating were presented by Collins at al.[52] and later by Friswell [53]. Differences between measure data and model predictions may arise due to randomness present in the system, e.g. manufacturing variability as well as to variations in the material properties of the structure components. In Friswell's

3

paper [53], errors in the analytical model and in the measurements (e.g. caused by noise [[27]]) are associated to a weighting matrix and it is shown how to estimate the variance in the updated parameters. This technique is called the minimum variance estimator. Other techniques for model updating in the presence of uncertainty are the Bayesian probabilistic framework presented by Beck, Katafygiotis, and Mares [54, 55, 56], model updating based on an inverse approach, and fuzzy arithmetic [57]. Soize[58] presented a methodology for robust model updating using a non-parametric probabilistic approach. Uncertainty in structural properties, such as Poisson's ratio, Young's modulus, mass density, modal damping, etc., are considered irreducible uncertainty and require different mathematical approaches for the updating procedure. The distributions of the updated parameters are then modified in order to improve the correlation between model-predicted distributions and measured data distributions. This is a technique developed by Mottershead at al., and Mare at al. [59, 56] and it is called stochastic model updating or uncertainty identification. The stochastic model updating is efficient, not only because it includes variability data due to measurement noise, for example, but also because it includes the variability already existing in the structural property [59, 56, 48, 49, 50]. Govers and Link[60] presented an approach for stochastic model updating with covariance matrix adjustment from uncertain experimental modal data. Further, researchers have investigated different problems using stochastic model updating [52, 53, 61, 62, 63] . The majority of those methods can include and estimate of the global model randomness or uncertainties that are assumed to be spatially homogeneous along the structure. By considering that structure parameter values can be spatially distributed in nature, Adhikari and Friswell [64] estimated distributed parameters modelled as realizations of a random field using modal parameters.

The main goal of this paper is to investigate the use of sensitivity-based model updating with measured FRFs to estimate spatially distributed parameters. The distributed parameters are assumed to be realizations of a random process, which is more realistic for simulating the variability caused by the man-

4

ufacturing process. The study uses a beam structure where the uncertainty is included in the flexural bending and mass per unit of length modelled by SEM. Such distributed deviations are unknown *a priori* and therefore can be considered to be samples from a random field, which is discretized into random variables using the KL expansion. The implemented technique is validated in a numerical simulation and then applied to experimental data for a polymer beam manufactured by 3D printing.

2. Spectral element method for stochastic systems

By supposing a linear damped distributed parameter dynamic system governed by a linear differential equation [65]

$$\rho_0 \frac{\partial^2 \mathbf{U}(\mathbf{r}, t)}{\partial t^2} + L_{10} \frac{\partial \mathbf{U}(\mathbf{r}, t)}{\partial t} + L_{20} \mathbf{U}(\mathbf{r}, t) = 0 \tag{1}$$

where $\mathbf{U}(\mathbf{r}, t)$ is the time dependent displacement variable, $\mathbf{r} \in \mathbb{R}$ is the spatial position vector, and t is time specified in some domain $\mathcal{D}$. In the frequency domain we can write eq. 1 as :

$$-\omega^2 \rho_0 \mathbf{u}(\mathbf{r}, \omega) + i\omega L_{10}\{\mathbf{u}(\mathbf{r}, \omega)\} + L_{20}\{\mathbf{u}(\mathbf{r}, \omega)\} = 0 \tag{2}$$

Similar to FEM, the frequency-dependent displacement within an element can be interpolated from the nodal displacements $u_e(\mathbf{r}, \omega) = \mathbf{g}(\mathbf{r}, \omega)^T \hat{\mathbf{u}}_e(\omega)$, where $\hat{\mathbf{u}}_e(\omega)$ is the nodal displacement vector and $\mathbf{g}(\mathbf{r}, \omega)$ is the vector of frequency-dependent shape functions represented by

$$\mathbf{g}(\mathbf{r}, \omega) = \mathbf{\Gamma}(\omega)\mathbf{s}(\mathbf{r}, \omega) \tag{3}$$

where $\mathbf{\Gamma}(\omega)$ is a complex matrix that depends on the boundary conditions and $\mathbf{s}(\mathbf{r}, \omega)$ is a vector containing exponential functions $[e^{-ik(\omega)x}]$. One of the advantages using SEM is that only one element is required for a homogeneous structural member. The global dynamic spectral matrix for a undamped deterministic system can be described as

$$D_0(\omega) = -\omega^2 \mathbf{M}(\omega) + \mathbf{K}(\omega) \tag{4}$$

In a weak form, frequency-dependent $n \times n$ complex stiffness and mass matrices can be expressed as

$$K(\omega) = \int_{\mathcal{D}} k_s(\mathbf{r}) L_{20}\{\mathbf{g}(\mathbf{r}, \omega)\} L_{20}\{\mathbf{g}(\mathbf{r}, \omega)\}^T dr \qquad (5)$$

and

$$M(\omega) = \int_{\mathcal{D}} \rho(\mathbf{r}) \mathbf{g}(r, \omega) \mathbf{g}(r, \omega)^T dr \qquad (6)$$

In this present work a spectral element for a straight homogeneous beam is used ([6, 7, 5]) and expanded for a stochastic treatment.

2.1. Spectral Beam Element

The fundamental equations for the flexural motion of a beam structure are briefly described. A more extensive formulation can be found in [6, 7]. Figure (1) shows an elastic two-node beam element with an uniform rectangular cross-section subjected to dynamic forces at both ends. In this section all parameters are assumed to be deterministic variables.
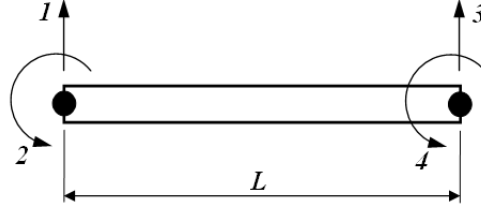

Figure 1: Two-node beam spectral element

The equation of motion of a damped Euler-Bernoulli beam under bending vibration may be written as [5],

$$\frac{\partial^2}{\partial x^2}\left[EI(x)\frac{\partial^2 v(x,t)}{\partial x^2}\right] + \rho A(x)\frac{\partial^2 v(x,t)}{\partial t^2} = 0 \qquad (7)$$

where EI is the bending stiffness, ρA is the mass per unit length, $v(x,t)$ is the transverse flexural displacement, E is the Young's modulus, A is the cross-section area, ρ is the mass density, and I is the inertia moment. A hysteretic

6

structural damping is assumed and introduced into the model formulation by adding an imaginary part proportional to the loss factor η to the Young's modulus. In the deterministic case a complex value given $E = E_0(1 + i\eta)$, where E_0 is the Young's modulus mean value, η is the loss factor and $i = \sqrt{-1}$ [6]. In the stochastic case, the complex random variable $E(\theta)$ will follow the complex random variable rules [21]. It is given by $E(\theta) = \hat{E}(\theta) + E_0 i\eta$, where the random part of the Young's modulus is a real value , $\hat{E}(\theta)$, and the imaginary part is taken as deterministic $E_0 i\eta$.

By considering the homogeneous differential equation with constant properties along the beam length, the spectral form becomes:

$$\frac{d^4\hat{v}}{dx^4} - \beta^4\hat{v} = 0 \tag{8}$$

Equation (8) can be split into a product of two terms which must vanish. A solution of the type $v(x)e^{i\omega t} = e^{kx}e^{i\omega t}$, where k (wavenumber) is given by:

$$k^4 - \beta^4 = 0 \quad \Rightarrow \quad k = \pm i\beta \, or \pm \beta \tag{9}$$

for

$$\beta^4 = \frac{\rho A \omega^2}{EI} \tag{10}$$

where ω is the circular frequency. For the spectral Euler-Bernoulli beam element of length L, the general solution of $v(x)e^{i\omega t} = e^{kx}e^{i\omega t}$ can be then obtained in the form of

$$v(\mathbf{x}, \omega) = a_1 e^{-ikx} + a_2 e^{-kx} + a_3 e^{-ik(L-x)} + a_4 e^{-k(L-x)} = \mathbf{s}(x, \omega)\mathbf{a} \tag{11}$$

where

$$\mathbf{s}(x, \omega) = \left[e^{-ikx}, e^{-kx}, e^{-ik(L-x)}, e^{-k(L-x)} \right]$$
$$\mathbf{a}(x, \omega) = \{a_1, a_2, a_3, a_4\}^T \tag{12}$$

The spectral nodal displacements and slopes of the beam element

$$\mathbf{d} = \begin{bmatrix} v_1 \\ \Theta_1 \\ v_2 \\ \Theta_2 \end{bmatrix} = \begin{bmatrix} v(0) \\ v'(0) \\ v(L) \\ v'(L) \end{bmatrix} \tag{13}$$

7

can be related to the displacement field at the two nodes ($x = 0$ and $x = L$), by

$$\mathbf{d} = \begin{bmatrix} s(0,\omega) \\ s'(0,\omega) \\ s(L,\omega) \\ s'(L,\omega) \end{bmatrix} \mathbf{a} = \mathbf{\Gamma}(\omega)\mathbf{a} \tag{14}$$

where

$$\mathbf{\Gamma}(\omega) = \begin{bmatrix} 1 & 1 & e^{-ikL} & e^{-kL} \\ -ik & -k & ie^{-ikL}k & e^{-kL}k \\ e^{-ikL} & e^{-kL} & 1 & 1 \\ -ie^{-ikL}k & -e^{-kL}k & ik & k \end{bmatrix} \tag{15}$$

The frequency-dependent displacement within an element is interpolated from the nodal displacement vector $\mathbf{d}$ by eliminating the constant vector $\mathbf{a}$ from Eq.(13) and using Eq.(14) it can be expressed as

$$v(x,\omega) = \mathbf{g}(x,\omega)\mathbf{d} \tag{16}$$

where the shape function can be expressed as

$$\mathbf{g}(\mathbf{x},\omega) = \mathbf{s}(\mathbf{x},\omega)\mathbf{\Gamma}^{-1}(\omega) = \begin{Bmatrix} g_1(x) \\ g_2(x) \\ g_3(x) \\ g_4(x) \end{Bmatrix}^T \tag{17}$$

$$= \begin{Bmatrix} \frac{-2\cos(kx)-2\cosh(kx)+(1-i)(\cos(k((1+i)L-x))+i\cos(k((1+i)L-ix))+\cosh(k((1+i)L-x))+i\cosh(k((1+i)L-ix)))}{4\cos(kL)\cosh(kL)} \\ -\frac{2\sin(kx)+2\sinh(kx)+(1+i)(\sin(k((1+i)L-x))-\sin(k((1+i)L-ix))+\sinh(k((1+i)L-x))-\sinh(k((1+i)L-ix)))}{4k(\cos(kL)\cosh(kL)-1)} \\ \frac{\cos(k(L-x))-\cos(kx)\cosh(kL)+\cosh(k(L-x))-\cos(kL)\cosh(kx)+\sin(kx)\sinh(kL)-\sin(kL)\sinh(kx)}{2-2\cos(kL)\cosh(kL)} \\ \frac{\sin(k(L-x))-\cos(kx)\sinh(kL)+\cosh(kx)(\sinh(kL)-\sin(kL))+\cosh(kL)(\sin(kx)-\sinh(kx))+\cos(kL)\sinh(kx)}{2k(\cos(kL)\cosh(kL)-1)} \end{Bmatrix}^T$$

In the case of the Euler-Bernoulli beam, a generalized transverse displacement at an arbitrary point can be expressed as (Eq. 16),

$$v(x) = g_1(x)v_1 + g_2(x)\Theta_1 + g_3(x)v_2 + g_4(x)\Theta_2$$

The damping is assumed hysteric and for this reason only the (4x4) mass and (4x4) stiffness matrices will be determined in a weak form:

$$\mathbf{K}_0(\omega) = \int_0^L EI_0(x)\mathbf{g}''(x)\mathbf{g}''^T(x)dx \tag{18}$$

and

$$\mathbf{M}_0(\omega) = \int_0^L \rho A_0(x)\mathbf{g}(x)\mathbf{g}^T(x)dx \tag{19}$$

where $'$ express the spatial partial derivative. The stochastic beam spectral element is formulated as a random process expanded in a spectral KL decomposition.

2.2. Karhunen-Loève expansion

Since the equations of motion for the beam spectral element are written as partial differential equations, it would be very difficult to apply random fields directly to them. To overcome this difficulty the random field is discretized in terms of random variables. By doing this, many mathematical procedures can be used to solve the resulting discrete stochastic differential equations. The procedure applied here is a random field spectral decomposition using the KL expansion. Assuming that the spectral covariance function is finite, symmetric and positive definite, it can be represented by a spectral decomposition, similar to a Fourier series expansion. By using this concept a random field can be expressed as a generalized Fourier series,

$$\varpi(\mathbf{r}, \theta) = \varpi_0(\mathbf{r}) + \sum_{j=1}^{\infty} \xi_j(\theta)\sqrt{\lambda_j}\varphi_j(\mathbf{r}) \tag{20}$$

where $\varpi(\mathbf{r}, \theta)$ is a random field with covariance function $C_\varpi(\mathbf{r}_1, \mathbf{r}_2)$, θ denotes an element of the sample space Ω, so that $\theta \in \Omega$, and $\xi_j(\theta)$ are uncorrelated random variables. The subscript 0, in $\varpi_0(\mathbf{r})$ implies the corresponding deterministic part. The constants λ_j and functions $\varphi_j(\mathbf{r})$ are, respectively, eigenvalues and eigenfunctions satisfying the integral equation:

$$\int_{\mathcal{D}} C_\varpi(\mathbf{r}_1, \mathbf{r}_2)\varphi_j(\mathbf{r}_1)d\mathbf{r}_1 = \lambda_j\varphi_j(\mathbf{r}_2) \quad \forall j = 1, 2, ... \tag{21}$$

9

In this paper one dimensional spaces are considered. Since a Gaussian random field is representative of many physical systems and closed form expressions for the KL expansion exist, a Gaussian autocorrelation function with exponential decay will be assumed here. It can be expressed as,

$$C(x_1, x_2) = e^{-|x_1 - x_2|/\mathsf{b}} \tag{22}$$

where b is the correlation length, which is an important parameter to describe the random field. A random field can be expanded in a finite basis of deterministic functions and random variables if the correlation length is large compared with the domain under consideration; for more details, see [3]. An analytical solution in the interval $-\mathsf{a} < x < \mathsf{a}$ where it is assumed that the mean is zero, produces a random field as,

$$\varpi_1(x, \theta) = \sum_{j=1}^{\infty} \xi_j(\theta) \sqrt{\lambda_j} \varphi_j(x) \tag{23}$$

Defining $\mathsf{c} = 1/\mathsf{b}$, the corresponding eigenvalues and eigenfunctions for odd j are given by [3],

$$\lambda_j = \frac{2\mathsf{c}}{\omega_j^2 + \mathsf{c}^2}; \quad \varphi_j(x) = \frac{\cos(\omega_j \frac{L}{2})}{\sqrt{\mathsf{a} + \frac{\sin(2\omega_j \mathsf{a})}{2\omega_j}}} \quad \text{where} \quad \tan(\omega_j \mathsf{a}) = \frac{\mathsf{c}}{\omega_j} \tag{24}$$

and for even j are given by,

$$\lambda_j = \frac{2\mathsf{c}}{\omega_j^2 + \mathsf{c}^2}; \quad \varphi_j(x) = \frac{\sin(\omega_j \frac{L}{2})}{\sqrt{\mathsf{a} - \frac{\sin(2\omega_j \mathsf{a})}{2\omega_j}}} \quad \text{where} \quad \tan(\omega_j \mathsf{a}) = \frac{\omega_j}{-\mathsf{c}} \tag{25}$$

These eigenvalues and eigenfunctions will be used to obtain the stochastic dynamic stiffness matrices for beam spectral elements.

For practical applications, equation (23) is truncated with M terms, which can be selected based on the amount of information to be kept. Its value is also related with the correlation length and the number of eigenvalues kept, provided that they are arranged in decreasing order.

2.3. Stochastic beam spectral element

In this work the flexural bending $(EI(x))$ and mass per unit length $(\rho A(x))$ are considered as spatially distributed random variables. Therefore, the flexural

10

bending is assumed as a random field of the form:

$$EI(x,\theta) = EI_0[1 + \varepsilon_1 \varpi_1(x,\theta)] \tag{26}$$

and the mass per unit of length is assumed a random field as

$$\rho A(x,\theta) = \rho A_0[1 + \varepsilon_2 \varpi_2(x,\theta)] \tag{27}$$

The subscript 0 indicates the mean value, $0 < \varepsilon_i \ll 1 (i = 1, 2, ...)$ are deterministic constants and the random field $\varpi_i(x,\theta)$ is taken to have zero mean, unit standard deviation and covariance $R_{ij}(\xi)$. Since, $EI(x,\theta)$ and $\rho A(x,\theta)$ are strictly positive, $\varpi_i(x,\theta)(i = 1, 2, ...)$ is rigorously required to satisfy the probability condition $P[1 + \varepsilon_i \varpi_i(x,\theta) \leq 0] = 0$. This requirement would exclude the use of Gaussian models for these random fields. However, for small ε_i, it is expected that Gaussian models can still be used if the primary interest of the analysis is to estimate the first few response moments and not the response behaviour near tails of the probability distributions. Expanding the random fields $\varpi_1(x,\theta)$ and $\varpi_2(x,\theta)$ in a KL spectral decomposition one obtains the (4x4) stochastic dynamic stiffness matrix written as,

$$\mathbf{D}(\omega,\theta) = \mathbf{D}_0(\omega) + \Delta\mathbf{D}(\omega,\theta)$$
$$= -\omega^2 \left[\mathbf{M}_0(\omega) + \Delta\mathbf{M}(\omega,\theta)\right] + \left[\mathbf{K}_0(\omega) + \Delta\mathbf{K}(\omega,\theta)\right] \tag{28}$$

where the deterministic part is given by the Eqs.(18)-(19), and the random part $\Delta\mathbf{D}(\omega,\theta)$ is related to the stiffness and mass coefficients $\Delta\mathbf{K}(\omega,\theta)$ and $\Delta\mathbf{M}(\omega,\theta)$, respectively, expanded in a KL decomposition of the form

$$\Delta\mathbf{K}(\omega,\theta) = \varepsilon_1 \sum_{j=1}^{N_K} \xi_{Kj}(\theta)\sqrt{\lambda_{Kj}}\mathbf{K}_j(\omega) \tag{29}$$

and

$$\Delta\mathbf{M}(\omega,\theta) = \varepsilon_2 \sum_{j=1}^{N_M} \xi_{Mj}(\theta)\sqrt{\lambda_{Mj}}\mathbf{M}_j(\omega) \tag{30}$$

where N_k and N_M are the numbers of terms kept in the KL expansion; $\xi_{Kj}(\theta)$ and $\xi_{Mj}(\theta)$ are uncorrelated Gaussian random variables with zero mean and

unit standard deviation. The constant (4x4) matrices $\mathbf{K}_j(\omega)$ and $\mathbf{M}_j(\omega)$ can be expressed as

$$\mathbf{K}_j(\omega) = EI_0 \int_0^L \varphi_{Kj}(x_e + x)\mathbf{g}''(x)\mathbf{g}''^T(x)dx \qquad (31)$$

$$\mathbf{M}_j(\omega) = \rho A_0 \int_0^L \varphi_{Kj}(x_e + x)\mathbf{g}(x)\mathbf{g}^T(x)dx \qquad (32)$$

where x_e the local coordinate. Substituting equation (24) and (25) in equation (31) and (32), the closed-form expressions for the random part of the stiffness and mass matrices for the beam spectral element in odd j can be expressed as

$$\mathbf{K}_j(\omega) = \frac{EI_0}{\sqrt{\mathsf{a} + \frac{\sin(2\omega_j \mathsf{a})}{2\omega_j}}} \left[\int_0^L \cos(\omega_j(x_e + x))\mathbf{g}''(x)\mathbf{g}''^T(x)dx \right] \qquad (33)$$

$$\mathbf{M}_j(\omega) = \frac{\rho A_0}{\sqrt{\mathsf{a} + \frac{\sin(2\omega_j \mathsf{a})}{2\omega_j}}} \left[\int_0^L \cos(\omega_j(x_e + x))\mathbf{g}(x)\mathbf{g}^T(x)dx \right] \qquad (34)$$

and for even j it is given by

$$\mathbf{K}_j(\omega) = \frac{EI_0}{\sqrt{\mathsf{a} - \frac{\sin(2\omega_j \mathsf{a})}{2\omega_j}}} \left[\int_0^L \sin(\omega_j(x_e + x))\mathbf{g}''(x)\mathbf{g}''^T(x)dx \right] \qquad (35)$$

$$\mathbf{M}_j(\omega) = \frac{\rho A_0}{\sqrt{\mathsf{a} - \frac{\sin(2\omega_j \mathsf{a})}{2\omega_j}}} \left[\int_0^L \sin(\omega_j(x_e + x))\mathbf{g}(x)\mathbf{g}^T(x)dx \right] \qquad (36)$$

3. Sensitivity-based updating method using FRFs

The objective of sensitivity based parameter estimation methods is to improve the correlation between the measured and predicted responses. The correlation is determined by an objective function involving modal or dynamic response data. In general, they are non-linear functions with respect to the model parameters, and so an iterative procedure is required with the possible associated convergence problems [27]. The non-linear least squares method uses a truncated Taylor series expansion of the dynamic response in terms of the

unknown parameters, often limited to the first two series terms, yielding the linear approximation:

$$\delta \mathbf{H} = \mathbf{S}_j \delta \xi, \tag{37}$$

where $\delta \mathbf{H} = \mathbf{H}_m - \mathbf{H}_j$ is the residual of the measured output, $\delta \xi = \xi - \xi_j$ is the perturbation in the parameters, and $\mathbf{S}_j$ is the sensitivity matrix. It contains the derivatives of the frequency response functions with respect to the chosen parameters to be varied, ξ_j. The iteration is initialized with ξ_0 equal to 0 and it is assumed that there are more measured data than unknown parameters. Then, equation (37) provides an over-determined set of simultaneous equations that can be solved using a least squares solution. Adopting the weighted objective function:

$$J(\delta \xi) = \varepsilon^T \mathbf{W}_e \varepsilon, \tag{38}$$

where $\varepsilon = \delta \mathbf{H} - \mathbf{S}_j \delta \xi$ is the error in the predicted measurements based on the updated parameters and $\mathbf{W}_e$ is a positive definite weighting matrix. Substituting ε in equation (38) leads to

$$J(\delta \xi) = \mathbf{W}_e \delta \mathbf{H} \delta \mathbf{H}^T - \mathbf{W}_e (\mathbf{S}_j \delta \mathbf{H}^T \delta \xi + \mathbf{S}_j^T \delta \mathbf{H} \delta \xi^T) + \delta \xi \mathbf{S}_j \mathbf{W}_e \mathbf{S}_j^T \delta \xi^T. \tag{39}$$

Minimizing J with respect to $\delta \xi$ is equivalent to:

$$\nabla J(\delta \xi) = 0 = -\mathbf{S}_j \mathbf{W}_e \delta \mathbf{H}^T + \mathbf{S}_j \mathbf{S}_j^T \mathbf{W}_e \delta \xi, \tag{40}$$

and solving equation (40) for $\delta \xi$ results,

$$\delta \xi = [\mathbf{S}_j^T \mathbf{W}_e \mathbf{S}_j]^{-1} \mathbf{S}_j^T \mathbf{W}_e \delta \mathbf{H}. \tag{41}$$

Thus, the updated parameter can be obtained from:

$$\xi_{j+1} = \xi_j + [\mathbf{S}_j^T \mathbf{W}_e \mathbf{S}_j]^{-1} \mathbf{S}_j^T \mathbf{W}_e (\mathbf{H}_m - \mathbf{H}_j). \tag{42}$$

The solution of equation (42) can be ill-conditioned, which might be a central problem in this kind of method. The treatment of ill-conditioning is explained in [66, 67, 68, 69, 32]. Titurus and Friswell [70] presented a regularization

13

treatment within the context of sensitivity-based FE model updating, which is used in this paper. The method gives the updated parameter vector as:

$$\xi_{j+1} = \xi_j + [\mathbf{S}_j^T \mathbf{W}_e \mathbf{S}_j + \gamma^2 \mathbf{W}_p]^{-1} \{\mathbf{S}_j^T \mathbf{W}_e (\mathbf{H}_m - \mathbf{H}_j)\}. \tag{43}$$

The regularization parameter $\gamma \in [0\ 1]$ determines the relative weight between the regularized solution $(\|\xi_{j+1} - \xi_j\|)$ versus the corresponding residual norm $(\|\S_j(\xi_{j+1} - \xi_j) - (\mathbf{H}_m - \mathbf{H}_j)\|)$. The size of the regularisation parameter γ will provides the balance between the residual $(\|\mathbf{H}_m - \mathbf{H}_j\|)$ and the parameter change $(\xi_{j+1} - \xi_j)$. For γ too small the problem will be too close to the original ill-posed problem, while γ too large the problem solved will have little connection with the original problem [67]. Link [71] suggested the regularisation parameter γ^2 lies between 0 to 0.3. Accordingly, in this paper the regularization parameter was assumed as 0.3. The updated parameter is evaluated in an iterative process until convergence, which is determined when the change in parameters,$\|\xi_{j+1} - \xi_j\|$ or the FRF $\|\mathbf{H}_m - \mathbf{H}_j\|$ is sufficiently small.

The choice of the weighting matrices is a difficult subject, and estimated statistical properties can be employed [27]. Here, we use a solution procedure presented by Grafe [47] where no explicit statistical calculations of the weighting factors are required and the correlation coefficient $(X_s(\omega))$ is used directly as

$$[\diagdown\mathbf{W}_e\diagdown] = [\diagdown X_s(\omega)\diagdown] \tag{44}$$

The correlation coefficient is based on the Modal Assurance Criterion (MAC) theory [72, 73]. For any measured frequency the correlation coefficient is a correlation between the measured and predicted response vectors, given by

$$X_s(\omega) = \frac{\left|\{H_m(\omega)\}^H \{H_a(\omega)\}\right|^2}{(\{H_m(\omega)\}^H \{H_m(\omega)\})(\{H_a(\omega)\}^H \{H_a(\omega)\})} \tag{45}$$

where $H_m(\omega)$ and $H_a(\omega)$ are the measured and predicted FRF vectors at matching excitation/response locations, respectively. $X_s(\omega)$ assumes a value between zero $(X_s(\omega) = 0)$ that indicates no correlation exists and unity $(X_s(\omega) = 1)$ which signifies perfect correlation. The correlation coefficient is sensitive to discrepancies in the global deflection shape of the structure. However analogous

14

to the MAC, it is unable to detect scaling errors. A definition of parameter weighing matrix $(\mathbf{W}_p)$ was proposed by Link [74] and later by Mottershead and Foster [69]. Similar to the approach of Link[74], the parameter weighing matrix used here is expressed as

$$[^\diagdown\mathbf{W}_{p\diagdown}] = \frac{\|[w_e]\|_2}{max(diag([w_e]))}[^\diagdown diag([w_e])_\diagdown] \tag{46}$$

where $[w_e] = [[\mathbf{S}][^\diagdown\mathbf{W}_{e\diagdown}][\mathbf{S}]^T]^{-1}$.

3.1. Stochastic sensitivity of the FRF

The sensitivity method is based on the linearisation of the non-linear relationship between measurable outputs (modal data or frequency response functions) and the model parameters to be estimated [32]. By considering that in practice the measured raw data obtained from the experimental test are the FRF, in this paper the sensitivity of the FRF will be used. The coefficients of the KL expansion are assumed as uncertain parameters and will be estimated by Eq. (42). By following [40, 42, 46, 47] the deterministic FRF sensitivity related to a general parameter φ can be written as:

$$\frac{\partial\mathbf{H}(\omega)}{\partial\varphi} = -\mathbf{H}(\omega)\frac{\partial\mathbf{D}(\omega)}{\partial\varphi}\mathbf{H}(\omega) \tag{47}$$

where $\mathbf{H}(\omega) = \mathbf{D}^{-1}(\omega)$ is the inverse of the deterministic dynamic stiffness matrix. In the stochastic context, two techniques can be applied. The fist one estimates a random variable, $\varphi(\theta)$. The second one is associated with the parameter ξ_{Kj} of the KL expansion, which are the uncorrelated random variables of the random field. With the first approach equation (47) becomes:

$$\frac{\partial\mathbf{H}(\omega,\theta)}{\partial\varphi(\theta)} = -\mathbf{H}(\omega,\theta)\frac{\partial\mathbf{D}(\omega,\theta)}{\partial\varphi(\theta)}\mathbf{H}(\omega,\theta) \tag{48}$$

where $\mathbf{H}(\omega,\theta) = \mathbf{D}^{-1}(\omega,\theta)$, which is inverse of the stochastic dynamic stiffness matrix (eq.28). In the second approach, used in this paper, equation (47) is described by:

$$\frac{\partial\mathbf{H}(\omega,\theta)}{\partial\xi} = -\mathbf{H}(\omega,\theta)\left[\frac{\partial\mathbf{K}(\omega,\theta)}{\partial\xi_{Kj}} - \omega^2\frac{\partial\mathbf{M}(\omega,\theta)}{\partial\xi_{Mj}}\right]\mathbf{H}(\omega,\theta) \tag{49}$$

15

the derivative of $\mathbf{K}(\omega,\theta)$ and $\mathbf{M}(\omega,\theta)$ related to the parameter ξ_{Kj} produces:

$$\frac{\partial \mathbf{K}(\omega,\theta)}{\partial \xi_{Kj}(\theta)} = \varepsilon_1 \sqrt{\lambda_{Kj}} \mathbf{K}_j(\omega) \tag{50}$$

and

$$\frac{\partial \mathbf{M}(\omega,\theta)}{\partial \xi_{Mj}(\theta)} = \varepsilon_2 \sqrt{\lambda_{Mj}} \mathbf{M}_j(\omega) \tag{51}$$

Substituting equation (50) and (51) in (49),

$$\frac{\partial \mathbf{H}(\omega,\theta)}{\partial \xi(\theta)} = s_{ij} = -H(\omega) \left[\varepsilon_1 \sqrt{\lambda_{Kj}} \mathbf{K}_j(\omega) - \omega^2 \varepsilon_2 \sqrt{\lambda_{Mj}} \mathbf{M}_j(\omega) \right] H(\omega) \tag{52}$$

In this paper the sensitivities of the receptance FRFs ($\mathbf{H}(\omega,\theta)$) were taken in dB scale [75] with 1m/N reference. It can be shown that [75]

$$\frac{\partial(20 log_{10}) |\mathbf{H}(\omega,\theta)|}{\partial \xi(\theta)} \approx 8.6859 \left(\frac{\Re(\mathbf{H}(\omega,\theta)) \frac{\partial(\mathbf{H}(\omega,\theta))}{\partial \xi(\theta)} + \Im(\mathbf{H}(\omega,\theta)) \frac{\partial(\mathbf{H}(\omega,\theta))}{\partial \xi(\theta)}}{\Re(\mathbf{H}(\omega,\theta))^2 + \Im(\mathbf{H}(\omega,\theta))^2} \right) \tag{53}$$

The elements of the sensitivity matrix s_{ij} are given by equation (53) and the $N_K + N_M$ dimensional vector of updating parameters ξ is

$$\xi = [\xi_{K_1}, \xi_{K_2}...,\xi_{K_{N_K}} \quad \xi_{M_1}, \xi_{M_2}...,\xi_{M_{N_M}}]^T \tag{54}$$

The elements of the vector ξ are sampled from independent and identically distributed standard Gaussian random variables (i.e., with zero-mean and unit standard deviation) from the KL expansion. The parameter vector ξ will be estimated from the measured FRF and used to reconstruct the $EI(x,\theta)$ and $\rho A(x,\theta)$ random field realizations. Once the parameters ξ are obtained, the estimated FRF can be calculated as $\mathbf{H}(\xi)$.

4. Numerical and experimental tests

The objective is to show the efficiency of the developed technique. A free-free beam structure is considered and modelled by a two-node beam spectral element with variabilities considered for the beam flexural rigidity EI and for the mass per unit of length ρA. The measured FRF simulates the receptance FRF with an impact force excitation at node 1 and displacement response measured at

some points along the beam. The nominal physical properties and geometrical parameters of the beam are: $L = 0.33$ m, $h = 0.006$ m, $b = 0.018$ m, $\eta = 0.1$, $E = 1.198$ GPa, and $\rho = 1140$ kg/m^3. It is assumed that a variation of the value of EI and ρA can be modelled by a homogeneous Gaussian random field. For the numerical calculations we considered $\epsilon_1 = \epsilon_2 = 20\%$ of variation with a correlation length of $\mathtt{b} = L/3$.

Numerical cases

Two initial cases were carried out with noise-free simulated FRFs which are referred to as synthetic measured FRF. In the first case, an investigation of how the number of FRFs considered can increase the amount of information and yield more accurate parameter estimates. A random field estimation of the beam flexural rigidity and mass per unit of length was performed. The data was generated using 4 terms in the KL expansion, simulating a physically realistic property. We use the FRFs obtained at beam length positions $(0 * L)$, $(0.25 * L)$, $(0.70 * L)$, and (L) of the perturbed beam element. In this case, the objective is to reconstruct the distributed flexural rigidity (EI) function and mass per unit of length (ρA) from the synthetic measured FRFs obtained with a sample of the stochastic beam model.
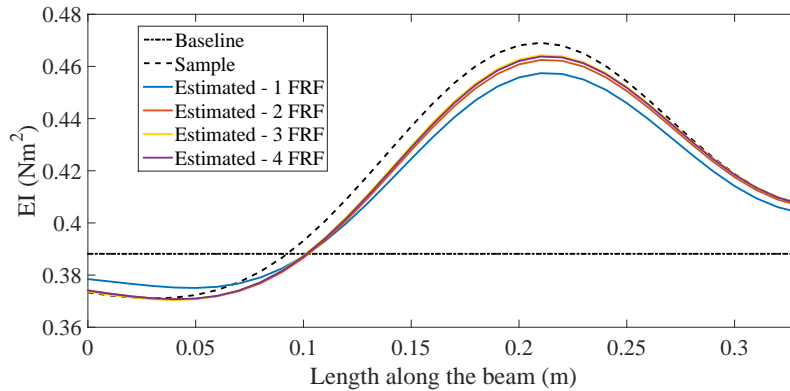
Figure 2: Baseline, sample and reconstructed random field sample of the flexural rigidity along the length using 1,2,3, and 4 FRFs in the estimation.
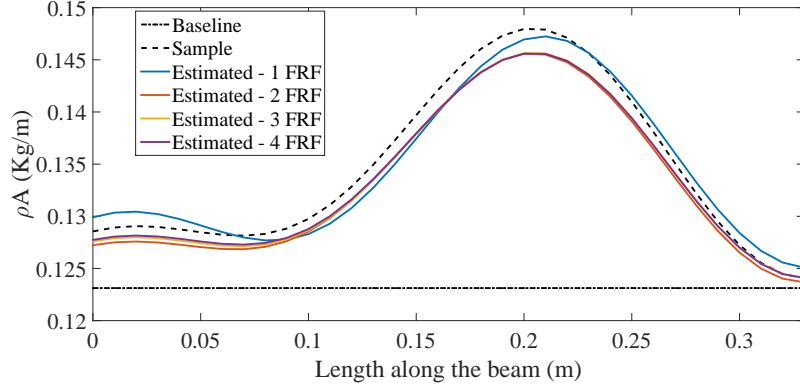
17

Figure 3: Baseline, sample and reconstructed random field sample of the mass per unit of length using 1,2,3, and 4 FRFs in the estimation.

The flexural rigidity random field sample estimated with 1, 2, 3 and 4 FRFs, and 4 terms in the KL expansion is shown in figure (2). In all cases, the re-
175 constructed functions are close to the simulated functions which generated the synthetic measured data. Analogously, the mass random field sample estimated is shown in figure (3). Both reconstructed random field samples using only one FRF showed the least effective estimation. By including FRFs in the updating procedure one can improve the information and a better estimation can be
180 achieved. In this numerical example, two FRFs are suitable for the analysis, given that the estimation using more than two FRFs did not present major improvements. Because of the increased information when more FRFs are included in the updating procedure, better estimation for the reconstructed random field samples were obtained.
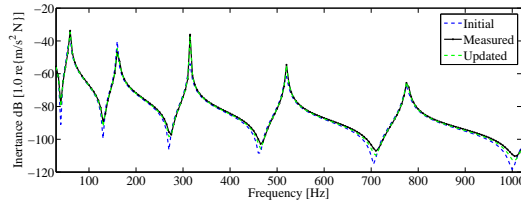
Figure 4: Comparison between the FRF obtained with an initial value, and updated value, and the synthetic measured FRF using one FRF at node $1(0 * L)$.
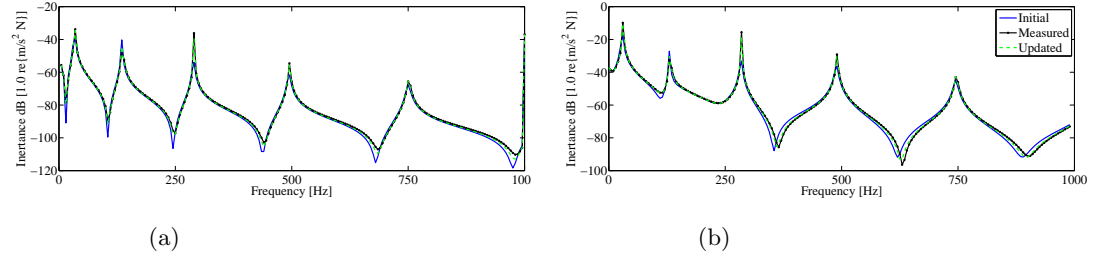
18

Figure 5: Comparison between an initial value, updated and the synthetic measured using two FRFs (a) at $0 * L$ and (b) at $0.25 * L$.
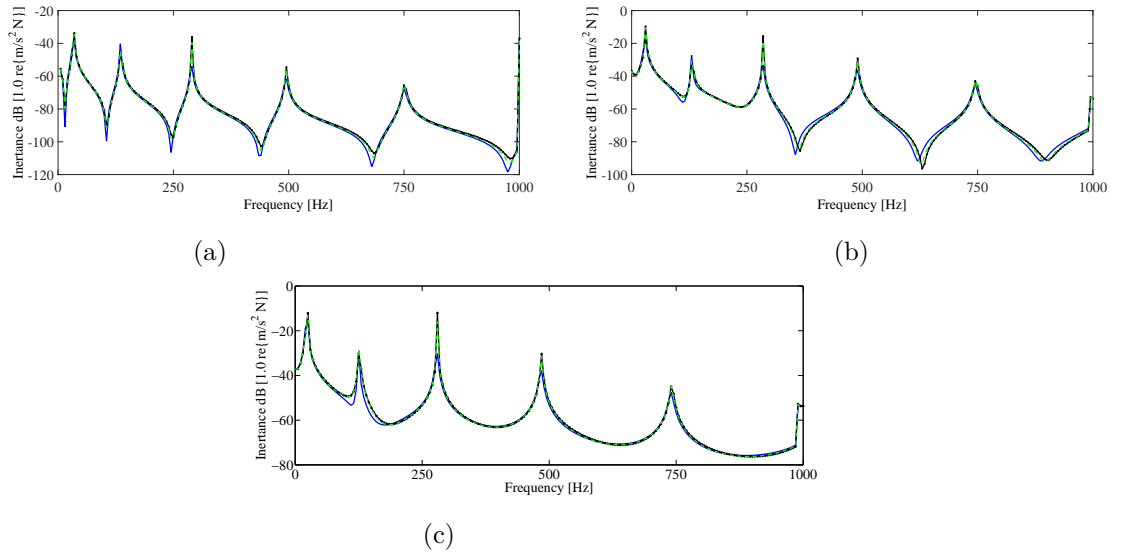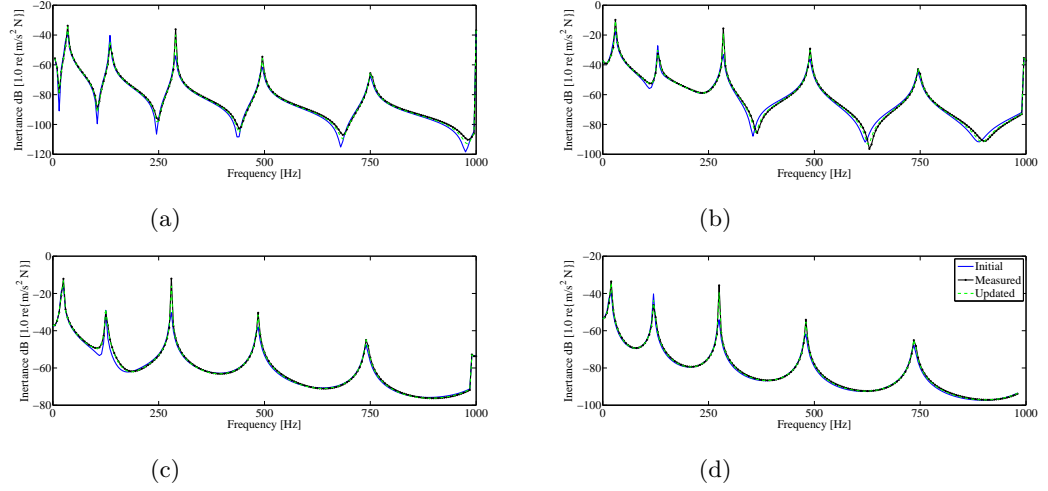

Figure 6: Comparison between an initial value, updated and the synthetic measured using three FRFs (a) at $0 * L$, (b) at $0.25 * L$, and (c) at $0.70 * L$.

The reconstructed random field samples are used to calculate the FRF of
the stochastic beam at each iteration in the optimisation procedure. The comparison between the synthetic measured, initial and updated FRF is shown in figure (4), (5), (6), and (7). In all cases of this first test (estimation with 1, 2, 3 and 4 FRFs), the initial FRFs are calculated assuming deterministic homogeneous EI and ρA, in the end of the iteration procedure the FRFs calculated

19

Figure 7: Comparison between an initial value, updated and the synthetic measured using four FRFs (a) at $0*L$, (b) $0.25*L$, (c) $0.70*L$, and (d) L.
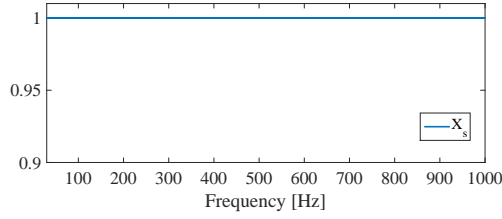

Figure 8: FRF correlation coefficient $(X_s(\omega))$.

with the estimated parameters is closer to the synthetic measured FRF. The FRFs exhibit a high level of correlation as it can be seen in the correlation co-efficients plotted in figure (8). The high correlation indicates no errors because of its immunity to scaling, i.e., each predicted frequency point can be scaled to match its measured counterpart. For all cases, similar correlation results were obtained.

20
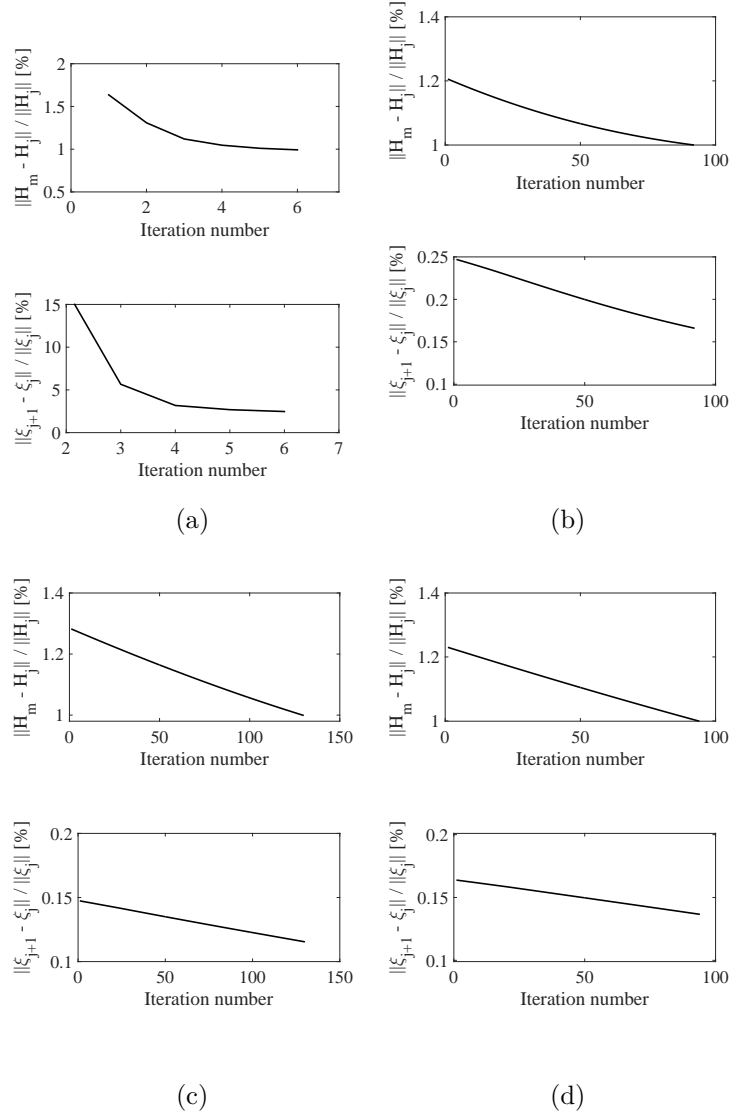
Figure 9: Convergence of the FRF residual ($\|\mathbf{H}_m - \mathbf{H}_j\|$) and parameters ($\|\xi_{j+1} - \xi_j\|$) using (a) 1 FRF, (b) 2 FRFs, (c) 3 FRFs, and (d) 4 FRFs.

The iteration convergence stop criterion was the change in the response, $\|\mathbf{H}_m - \mathbf{H}_j\|$ or change in parameter $\|\xi_{j+1} - \xi_j\|$ below 1% and 0,1% of relative error, respectively. Figure 9(a-d) shows the convergence of the FRFs and updating parameters estimated using 1 , 2, 3, and 4 FRFs.

In the second case, it was fixed in two the number of FRFs used in the estimation and varied the number of terms in the KL expansion. The FRFs used were measured at node 1 and 2. Two other samples of random field data were generated with 12 terms in the KL expansion. The estimation of distributed parameters, EI and ρA, was performed with 4, 8 and 12 terms in the expansion, and similar stop criteria was assumed. As in the last test, the objective is to reconstruct the distributed flexural rigidity and mass from the synthetic measured FRFs obtained with a sample of the stochastic model. However, the random field samples are estimated with a different number of terms.
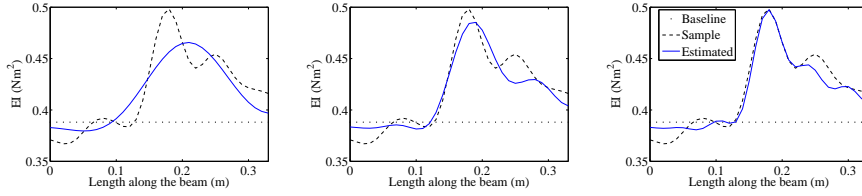

Figure 10: Baseline, sample and reconstructed random field sample of the flexural rigidity along the length using 4 (LHS), 8 (middle) and 12 (RHS) modes.
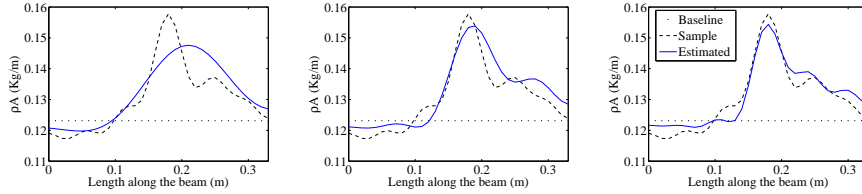

Figure 11: Baseline, sample and reconstructed random field sample of the mass along the length using 4 (LHS), 8 (middle) and 12 (RHS) modes.

Figures (10) and (11) show the flexural rigidity and mass random field sample estimations, respectively. As mentioned, the samples were simulated with 12 modes in the KL expansion and the estimation performed using 4 (shown in Fig. 11 on the left had side, 8 (shown in the middle), and 12 (shown in the right hand side) parameters (ξ). Although the terms in the KL expansion cannot be precisely estimated from the data, note that both reconstructed distributed random parameters presented a good approximation of the sample distributed

22

parameters. Obviously, the random field samples reconstructed with the same number as the actual sample can better represent the distributed parameter. However, the reconstruction performed with 4 and 8 modes was reasonable.
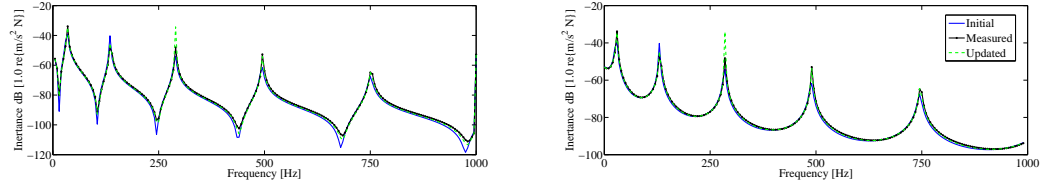

Figure 12: Comparison among an initial, updated and the synthetic measured FRF at node 1 (LHS) and node 2 (RHS). Updated FRFs calculated with the random field sample reconstructed with 4 modes.
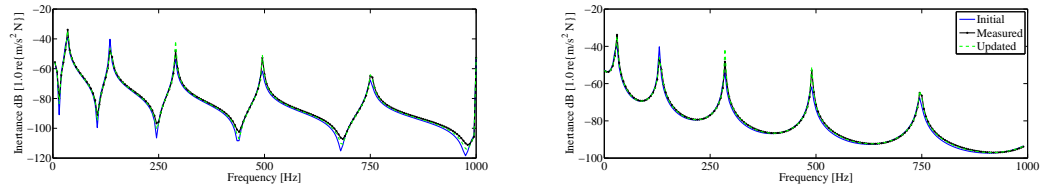

Figure 13: Comparison among an initial, updated and the synthetic measured FRF at node 1 (LHS) and node 2 (RHS). Updated FRFs calculated with the random field sample reconstructed with 8 modes.
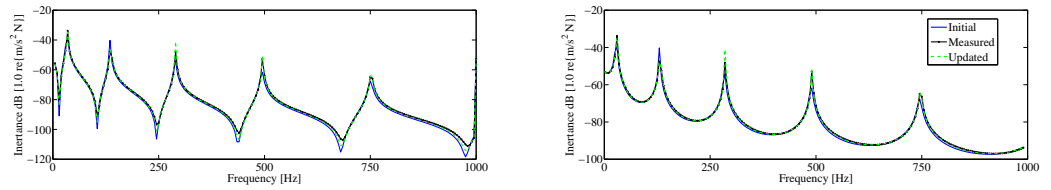

Figure 14: Comparison among an initial, updated and the measured FRF at node 1 (LHS) and node 2 (RHS). Updated FRFs calculated with the random field sample reconstructed with 12 modes.

Next, the reconstructed flexural rigidity EI and mass per unit of length ρA were used to calculate the frequency response function of the stochastic beam at each iteration of the optimization procedure. The responses used 4, 8 and 12
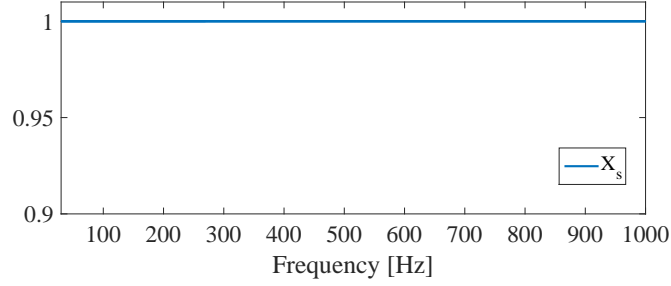
23

Figure 15: FRF correlation coefficient $(X_s(\omega))$.

terms in KL expansion, are shown in figures (12), (13) , and (14), respectively.
They show the comparison between initial, synthetic measured, and estimated
FRFs. In all cases, the comparison between the updated and synthetic measured
FRFs showed a suitable approximation. Figure (15) shows that the correlation
function $(X_s(\omega))$ is unity across the full spectrum. The major part of the correc-
tions was introduced by the first iterations and subsequent iterations introduced
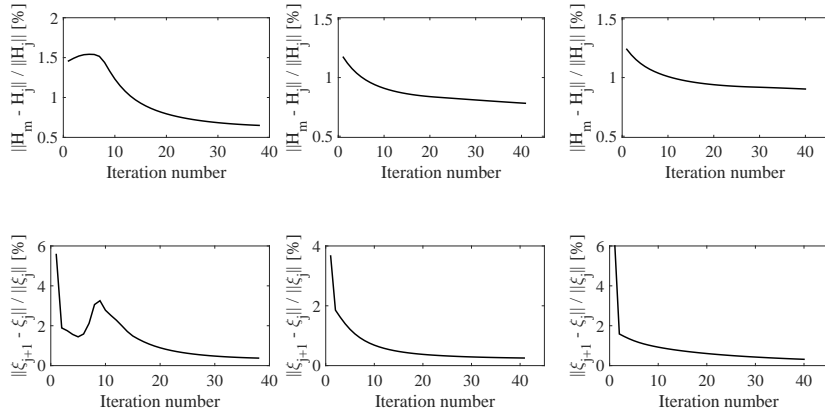only minor adjustments.

Figure 16: Convergence of the FRF $(\|\mathbf{H}_m - \mathbf{H}_j\|)$ and parameters $(\|\xi_{j+1} - \xi_j\|)$ using 4 (LHS),
8 (middle) and 12 (RHS) terms in the KL expansion.

In figure 16 the graphics show the evolution of the iteration process until
the change in the FRFs or change in the updating parameters with 4, 8, and 12
terms in KL expansion falls under a determined threshold value. In this case,

24

similar to the first case, the stop criterion was assumed 0.5% for both.

Experimental results

A beam made of polyamide (PA) with uniform rectangular cross-section was used in the experimental tests. The beam is 18mm wide, 6mm thick, with a mass per unit length of approximately 0.02343kg/m. The average flexural rigidity (EI) was obtained experimentally. The beam was manufactured using the Selective Laser Sintering (SLS) technology. As a consequence of the manufacturing process, a variability of the beam properties along its length can be expected. In order to verify the efficiency of the proposed method it was applied to a measured FRF and results were compared with measurements of the flexural rigidity at many points along the beam measured using an ultrasound apparatus. The Young's modulus (E) was measured at 22 points along the beam with an ultrasonic pulse-echo device. The experimental setup is shown in figure (17). In this experiment a shear wave transducer ($Olympus U8403072/U8403071$) was used. The signals were measured and analysed using an Olympus Parametrics NDT EPOCH 4 Ultrasonic Flaw Detector. The measured Young's modulus E along the beam is shown in figure (19), where it is compared with the predicted values using the KL expansion with 4 and 6 estimated parameters. The number of terms in KL expansion was chosen based on the shape sample characteristics.

Figure 17: Procedure for experimental measurement of polyamide beam properties.

Figure (18) shows the second experimental test setup, used to measure the FRFs. The signals were acquired and analysed using LMS Test Lab. The FRFs were estimated with a bandwidth of 1024Hz and 1024 spectral lines. An impact hammer was used to excite the structure and a micro accelerometer Kistler series 8614A was used to measure the response. The experimental FRFs were obtained by impact force excitation at node 1 and acceleration response at node 1 and node 2. The micro accelerometer mass is considerably small and lightweight compared with the beam so that the accelerometer mass was neglected. To simulate the free-free boundary condition we supported the beam by using a soft polyurethane foam edges.
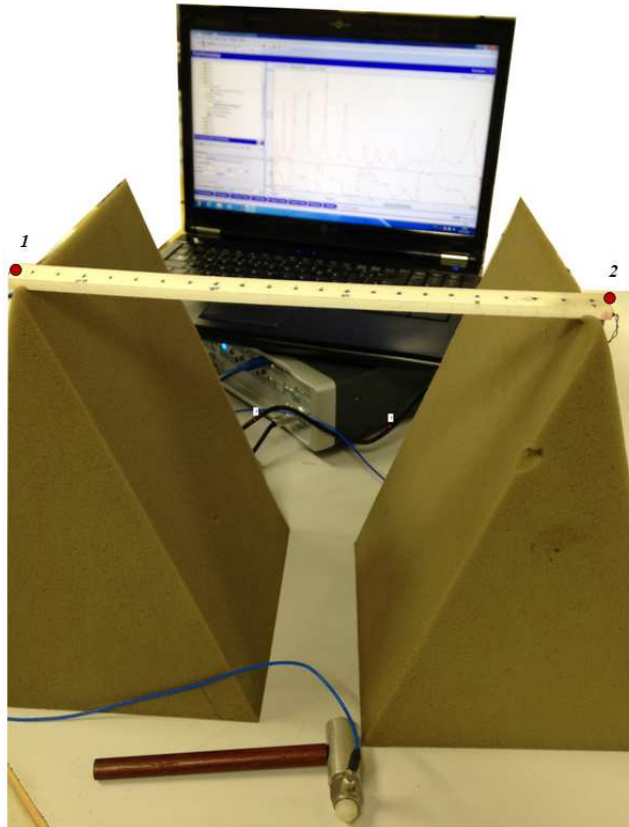
Figure 18: The test rig for the free-free beam.

The initial, measured sample of EI and reconstructed distributed sample with 4 and 6 terms in KL expansion are shown in figure (19). The random field experimental sample could not be reconstructed accurately; nevertheless, an acceptable difference between updated and measured FRFs can be observed. Experimental, initial and updated FRFs using 4 and 6 terms in KL expansion are illustrated in figure (20) and (21), respectively. Similar stop criteria of the numerical case were applied. Examining both cases, it can be observed that the reconstruction using 6 terms was more appropriated in this test. Even the FRFs updated procedure showed better convergence using 6 terms; However, the reconstructed $EI(x)$ with 4 terms presents a good approximation compared

with random field sample measured by ultrasound. Figure 23 shows the iteration process until the change in the FRFs and change in the updating parameters converge with 4, and 6 terms in the KL expansion.
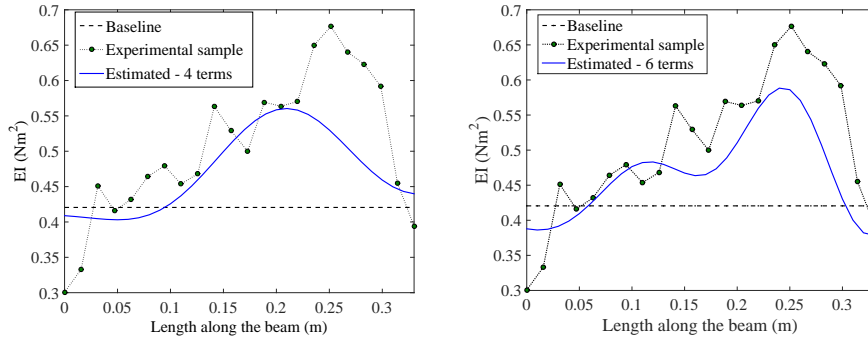

Figure 19: Baseline, experiential sample and reconstructed random field sample of the flexural rigidity ($EI(x)$) with 4 (LHS) and 6 (RHS) terms in the KL expansion.

Figure 20: Comparison between an initial value, updated and the experimental measured FRF at node 1 (LHS) and at node 2 (RHS) using 4 terms in the KL expansion.
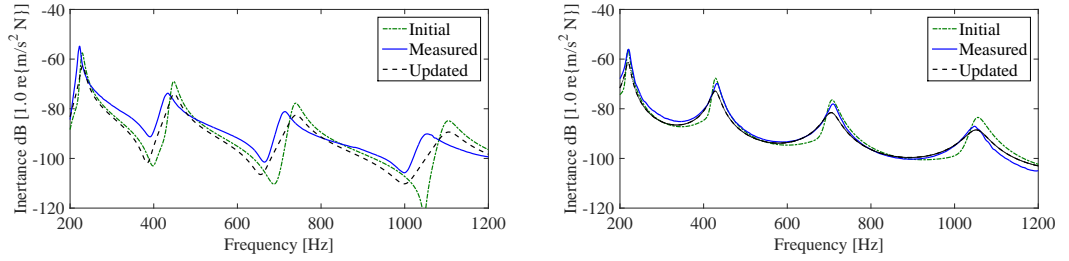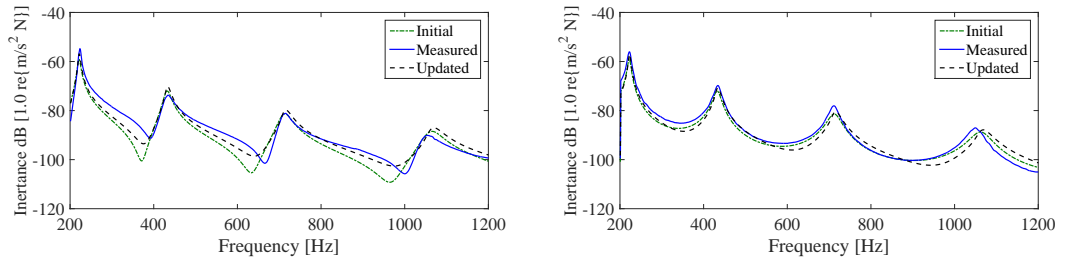

Figure 21: Comparison between an initial value, updated and the experimental measured FRF at node 1 (LHS) and at node 2 (RHS) using 6 terms in the KL expansion.
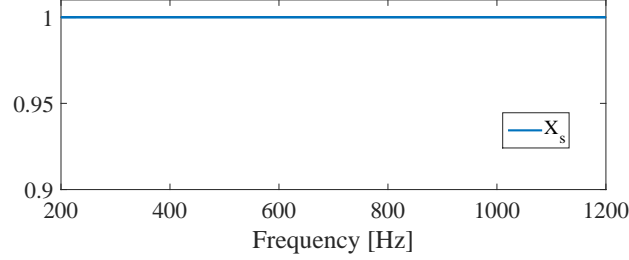
Figure 22: FRF correlation coefficient ($X_s(\omega)$).
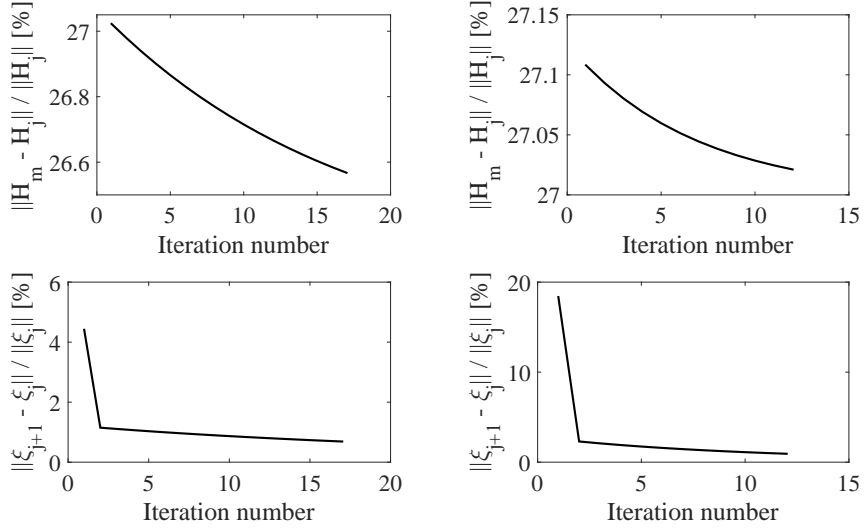
Figure 23: Convergence of the FRF ($\|\mathbf{H}_m - \mathbf{H}_j\|$) and parameters ($\|\xi_{j+1} - \xi_j\|$) using 4 (LHS) and 6 (RHS) terms in the KL expansion.

As shown in figure (22), the adjustments in the model have led to a high
level of correlation. Regarding the numerical and experimental cases presented, it was shown that the proposed method can be used to reconstruct the distributed variability of the beam. In all cases, the random field samples were reconstructed with a certain error associated. In general, all results were satisfactory; close shape of the random field sample was estimated, which demonstrated the performance of the proposed technique. It was also observed that the iteration always stopped after achieving the threshold value for the FRF

29

residual, similarly to the second case.

5. Final Remarks

In the present work, a technique to estimate spatially distributed parameters
of samples of a stochastic structure using a KL expansion and sensitivity-based
FRF model updating was proposed. Randomness was included in the flexural
rigidity (EI) and mass per unit length (ρA) of a beam structure. As a stochastic
model is employed, the sensitivity-based method using FRF is also developed
for a stochastic model based on a spectral beam element. To verify the efficiency
of the presented technique numerical and experimental tests were performed. In
the first case, random field estimation of the beam flexural bending and mass
per unit length have were performed. The discretized variables (ξ) were es-
timated from the synthetic measured FRF through a non-linear least squares
curve fit procedure. A subset of these random variables can be considered as
parameters to reconstruct the random field of the flexural bending and mass per
unit of length. In the experimental test, an experimentally obtained FRF was
used. An experimental measurement of Young's modulus at 22 points along
the beam was performed using ultrasound. By comparing the reconstructed
and experimentally measured of $EI(x)$ the proposed method proved to work
reasonably well. Ongoing work consists of improving these preliminary results
by curve fitting many measured FRF, instead of just one, to enrich the spatial
information of the measured data. Based on the numerical and experimental
cases presented, it was shown that the proposed method can be used to recon-
struct the distributed variability of the beam. In all cases, the random field
samples were reconstructed with a certain error associated. In general, all re-
sults were satisfactory, close shape of the random field sample was estimated,
which demonstrated the performance of the proposed technique.

References

[1] I. M. Sobol', A primer for the Monte Carlo method, CRC Press, 1994.

[2] D. Xiu, Numerical Methods for Computations-A Spectral method approcah, Princeton University Press, 2010.

[3] R. Ghanem, P. Spanos, Stochastic Finite Elements - A Spectral Approach, Sprin, 1991.

[4] G. Stefanou, The stochastic finite element method: Past, present and future, Computer Methods in Applied Mechanics and Engineering 198 (2009) 1031 – 1051.

[5] S. Adhikari, Doubly spectral stochastic finite-element method for linear structural dynamics, American Society of Civil Engineers 1 (2011) 264–276.

[6] J. F. Doyle, Wave propagation in structures : spectral analysis using fast discrete Fourier transforms, 2nd Edition, Mechanical engineering, Springer-Verlag New York, Inc., New York, 1997.

[7] U. Lee, Spectral Element Method in Structural Dynamics, BInha University Press, 2004.

[8] S. M. Hashemi, M. J. Richard, G. Dhatt, A new Dynamic Finite Element (DFE) formulation for lateral free vibrations of Euler-Bernoulli spinning beams using trigonometric shape functions, Journal of Sound and Vibration 220 (4) (1999) 601–624.

[9] S. M. Hashemi, M. J. Richard, Free vibrational analysis of axially loaded bending-torsion coupled beams: a dynamic finite element, Computer and Structures 77 (6) (2000) 711–724.

[10] M. Paz, Structural Dynamics: Theory and Computation, 2nd Edition, Van Nostrand, Reinhold, 1980.

[11] J. R. Banerjee, F. W. Williams, Exact bernoulli-euler dynamic stiffness matrix for a range of tapered beams, International Journal for Numerical Methods in Engineering 21 (12) (1985) 2289–2302.

[12] J. R. Banerjee, Coupled bending torsional dynamic stiffness matrix for beam elements, International Journal for Numerical Methods in Engineering 28 (6) (1989) 1283–1298.

[13] J. R. Banerjee, F. W. Williams, Coupled bending-torsional dynamic stiffness matrix for timoshenko beam elements, Computer and Structures 42 (3) (1992) 301–310.

[14] J. R. Banerjee, S. A. Fisher, Coupled bending torsional dynamic stiffness matrix for axially loaded beam elements, International Journal for Numerical Methods in Engineering 33 (4) (1992) 739–751.

[15] N. J. Ferguson, W. D. Pilkey, Literature review of variants of dynamic stiffness method, Part 1: The dynamic element method, The Shock and Vibration Digest 25 (2) (1993) 3–12.

[16] N. J. Ferguson, W. D. Pilkey, Literature review of variants of dynamic stiffness method, Part 2: Frequency-dependent matrix and other, The Shock and Vibration Digest 25 (4) (1993) 3–10.

[17] J. R. Banerjee, F. W. Williams, Free-vibration of composite beams - an exact method using symbolic computation, Journal of Aircraft 32 (3) (1995) 636–642.

[18] C. S. Manohar, S. Adhikari, Dynamic stiffness of randomly parametered beams, Probabilistic Engineering Mechanics 13 (1) (1998) 39–51.

[19] J. R. Banerjee, Dynamic stiffness formulation for structural elements: A general approach, Computer and Structures 63 (1) (1997) 101–103.

[20] S. Adhikari, C. S. Manohar, Transient dynamics of stochastically parametered beams, ASCE Journal of Engineering Mechanics 126 (11) (2000) 1131–1140.

[21] A. Papoulis, S. U. Pillai, Probability, random variables and stochastic processes., McGraw-Hill, Boston, 2002.

[22] F. Poirion, C. Soize, Monte carlo construction of karhunen-loeve expansion for non-gaussian random fields, in: Proceedings of the 13th ASCE Engineering Mechanics Division Conference, 1999.

[23] P. F. Puig, B., C. Soize, Non-gaussian simulation using hermite polynomial expansion: convergences and algorithms, Probabilistic Engineering Mechanics 17(3) (2002) 253Dc264. `doi:10.1016/S0266-8920(02)00010-3`.

[24] S. Sakamoto, R. Ghanem, Simulation of multi-dimensional non-gaussian non-stationary random fields, Probabilistic Engineering Mechanics 17(2).

[25] K. K. Phoon, H. W. Huang, S. T. Quek, Simulation of strongly non-gaussian processes using karhunen-loeve expansion, Structural Safety 20(2) (2005) 1881198. `doi:10.1016/j.probengmech.2005.05.007`.

[26] J. E. Mottershead, M. Friswell, Model updating in strucutral dynamics: A survey, Journal of Sound and Vibration 167(2) (1993) 347– 375.

[27] M. I. Friswell, J. E. Mottershead, Finite element model updating in structural dynamics, Kluwer Academic Publishers, 1995.

[28] M. Link, O. Santiago, Updating and localizing structural errors based on minimization of equation errors, in: In International Conference on Spacecraft Structures and Mechanical Testing (ESA/ESTEC), 1991.

[29] J. Mottershead, M. Friswell, G. Ng, J. Brandon, Geometric parameters for finite element model updating of joints and constraints, Mechanical Systems and Signal Processing 10(2) (1996) 171–182.

[30] G. Gladwell, H. Ahmadian, Generic element matrices suitable for finite element updating, Mechanical Systems and Signal Processing 9(6) (1996) 601–614.

[31] M. I. Friswell, J. Mottershead, H. Ahmadian, Combining subset selection and parameter constraints in model updating, ASME Journal of Vibration and Acoustics 120(4) (1998) 854–859.

[32] J. E. Mottershead, M. Link, M. I. Friswell, The sensitivity method in finite element model updating: A tutorial, Mechanical Systems and Signal Processing 25 (2011) 2275–2296.

[33] D. J. Ewins, Modal Testing: Theory and Practice, Research Studies Press, 1984.

[34] N. M. Maia, M. Julio, Theoretical and Experimental Modal Analysis, Research Studies Pre, 1997.

[35] S. Modak, K. Kundra, B. Nakra, Prediction of dynamic characteristic using updated finite element models., Journal of Sound and Vibration 254(3) (2002) 447–467.

[36] M. I. Friswell, Using vibration data and statistical measures to locate damage in structures, Modal Anal. Int. J. Anal. Exp. Modal Anal. 9 (1994) 239–254.

[37] J. Mottershead, C. Mares, M. Friswell, S. James, Selection and updating of parameters for an aluminium space-frame model., Mechanical Systems and Signal Processing 14(6) (2000) 923–944. doi:doi.org/10.1006/mssp.2000.1303.

[38] H. Ahmadian, J. E. Mottershead, S. James, M. I. Friswell, C. A. Reece, Modelling and updating of large surface-to-surface joints in the awe-mace structure, Mechanical Systems and Signal Processing 20(4) (2006) 868–880.

[39] N. M. M. Maia, J. M. M. Silva (Eds.), Theoretical and Experimental Modal Analysis, Engineering Dynamics Series, Research Studies Press, Taunton, England, 1997, series Editor, J. B. Robetrs.

[40] H. Natke, Die korrektur des rechenmodells eines elastomechanischen systems mittels gemessener erzwungener schwingungen, Ingenieur-Archiv 46 (1977) 169–184.

[41] H. Natke, Updating computational models in the frequency domain based on measured data: a survey, Probabilistic Engineering Mechanics 3 (1988) 28–35.

[42] N. Cottin, H. Felgenhauer, H. G. Natke, On the parameter identification of elastomechanical systems using inout and output residuals, Ingenieure Archiv 54(5) (1984) 378–387.

[43] M. Link, Identification and correction of errors in analytical models using test data theoretical and practical bounds, in: In International Conference on Space- craft Structures and Mechanical Testing (ESA/ESTEC), 1990.

[44] S. R. Ibrahim, W. DAmbrogio, P. Salvini, S. Sestieri, Direct updating of nonconservative finite element models using measured input - output, in: In 10th International Modal Analysis Conference, San Diego, USA, 1992.

[45] H. Natke, Einfuhrung in in Theorie und Praxis der Zeitreihen und Modalanalyse,, Vieweg Verlag, 1992.

[46] J. Arruda, J. D. Santos, Mechanical joint paramenter estimation using frequency response function and component mode synthesis, Mechanical Systems and Signal Processing 7(6) (1993) 493–508.

[47] H. Grafe, Model updating of large structural dynamics models using measured response functions, Ph.D. thesis, Imperial College of Science, Technology and Medicine University of London Model (1998).

[48] H. H. Khodaparast, J. Mottershead, Efficient methods in stochastic model updating, in: Proceedings of ISMA, 2008.

[49] H. H. Khodaparast, J. E. Mottershead, M. I. Friswell, Perturbation methods for the estimation of parameter variability in stochastic model updating, Mechanical System and Signal Processing 22 (8) (2008) 1751–1773.

[50] H. Khodaparast, Stochastic finite element model updating and its application in aeroelasticity, Ph.D. thesis, University of Liverpool (2010).

[51] O. A. Vanli, S. Jung, Statistical updating of finite element model with lamb wave sensing data for damage detection problems, Mechanical Systems and Signal Processing.

[52] J. D. Collins, G. C. Hart, T. K. Hasselman, B. Kennedy, Statistical identification of structures, AIAA Journal 2 (1974) 185–190. doi:ISI:A1974S090700010.

[53] M. I. Friswell, The adjustment of structural parameters using a minimum variance estimator, Mechanical Systems and Signal Processing 3 (1989) 143–155. doi:10.1016/0888-3270(89)90013-7.

[54] J. L. Beck, L. S. Katafygiotis, Updating models and their uncertainties. I: bayesian statistical framework, Journal of Engineering Mechanics 124 (4) (1998) 455–461.

[55] L. S. Katafygiotis, J. L. Beck, Updating models and their uncertainties. II: model identifiability, Journal of Engineering Mechanics 124 (4) (1998) 463–467.

[56] C. Mares, J. E. Mottershead, M. I. Friswell, Stochastic model updating: part 1 - theory and simulated example, Mechanical System and Signal Processing 20 (7) (2006) 1674–1695.

[57] T. Haag, J. Herrmann, M. Hanss, Identification procedure for epistemic uncertainties using inverse fuzzy arithmetic, Mechanical Systems and Signal Processing 24(7) (2010) 2021–2034.

[58] C. Soize, Robust updating of uncertain computational models using experimental modal analysis, AIAA Journal 46(11) (2008) 2955–2965.

[59] J. Mottershead, C. Mares, S. James, M. Friswell, Stochastic model updating: Part 2: Application to a set of physical structures, Mechanical Systems and Signal Processing 20(8) (2006) 2171–2185.

[60] Y. Govers, M. Link, Stochastic model updating covariance matrix adjustment from uncertain experimental modal data, Mechanical Systems and Signal Processing 24(3) (2010) 696–706. doi:10.1016/j.ymssp.2009.10.006.

[61] J. Beck, S. Au, Bayesian updating of structural models and reliability using markov chain monte carlo simulation, Journal of Engineering Mechanics 128(4) (2002) 380–391.

[62] J. R. Fonseca, M. I. Friswell, J. E. Mottershead, A. W. Lees, Uncertainty identification by the maximum likelihood method, Journal of Sound and Vibration 288 (3) (2005) 587–599.

[63] X. Hua, Y. Ni, Z. Chen, J. Ko, An improved perturbation method for stochastic finite element model updating, International Journal for Numerical Methods in Engineering 73(13) (2008) 1845–1864.

[64] S. Adhikari, M. Friswell, Distributed parameter model updating using the karhunen-loève expansion, Mechanical Systems and Signal Processing 24 (2010) 326–339.

[65] L. Meirovitch, Principles and techniques of vibrations, Prentice-Hal, 1997.

[66] M. I. Friswell, J. E. Mottershead, H. Ahmadian, Finite element model updating using experimental test data: parametrization and regularization, Philosophical Transactions of The Royal Society of London Series A - Mathematical Physical and Engineering Sciences 359 (1778) (2001) 169–186.

[67] H. Ahmadian, J. Mottershead, M. Friswell, Regularisation methods for finite element model updating, Mechanical Systems and Signal Processing 1 (1998) 47–64.

[68] M. Friswell, J. Mottershead, H. Ahmadian, Finite element model updating using experimental test data: parameterisation and regularisation, Transactions of the Royal Society of London, Series A: Mathematical, Physical and Engineering Sciences 359 (2001) 169–186.

[69] J. E. Mottershead, C. D. Foster, On the treatment of ill-conditioning in spatial parameter estimation from measured vibration data, Mechanical Systems and Signal Processing 5(2) (1991) 139–154.

[70] B. Titurus, M. Friswell, Regularization in model updating, International Journal for Numerical Methods in Engineering 75 (2008) 440–478.

[71] M. Link, Updating of analytical models procedures and experiments., Conference on Modern Practice in Stress and Vibration Analysis (April 1993) 35–52.

[72] R. Allemang, D. Brown, A correlation coefficient for modal vector analysis, in: 1st International Modal Analysis Conference, Orlando, USA., 1982.

[73] R. Allemang, The modal assurance criterion (mac): Twenty years of use and abuse, in: IMAC-XX:Conference & Exposition on Structural Dynamics, 2002.

[74] M. Link, Updating analytical models by using local and global parameters and relaxed optimisation requirements, Mechanical Systems and Signal Processing 12 (1998) 7–22.

[75] J. Arruda, Objective functions for the nonlinear curve-fit of frequency response functions, AIAA Journal 30(3) (1992) 855–857.